scientific reports

Check for updates

OPEN

Multiparametric ultrasound assessment of axillary lymph nodes in patients with breast cancer

Katarzyna Dobruch-Sobczak[1,2]✉, Axana Szlenk[1], Magdalena Gumowska[1], Joanna Mączewska[1], Katarzyna Fronczewska[1], Ewa Łukasiewicz[1], Katarzyna Roszkowska-Purska[3] & Magda Jakubczak[1]

The presence and extent of metastatic disease in axillary lymph nodes (ALNs) in the setting of breast cancer (BC) are important factors for staging and therapy planning. The purpose of this study was to perform a multiparametric sonographic evaluation of ALNs to better differentiate between benign and metastatic nodes. Ninety-nine patients (mean age 54.1 y) with 103 BCs were included in this study, and 103 ALNs were examined sonographically. B-mode parameters, such as size in two dimensions, shape, cortical thickness and capsule outline, were obtained, followed by vascularity assessment via colour Doppler and microflow imaging and stiffness evaluation via shear wave elastography. Postoperative histopathological evaluation was the reference standard. In the statistical analysis, logistic regression and ROC analyses were conducted to search for feature patterns of both types of ALNs to evaluate the prediction qualities of the analysed variables and their combinations. For a cortex larger than 3 mm, without a circumscribed margin of the LN capsule and SWE (E max > 26 kPa), the AUC was 0.823. Multiparametric assessment, which combined conventional US, quantitative SWE and vascularity analysis, was superior to the single-parameter approach in the evaluation of ALNs.

Axillary lymph node ultrasonography (ALNUS) is routinely performed in patients with breast cancer (BC) during preoperative evaluation[1,2]

The presence of metastases in the axillary lymph nodes (ALNs) and the number and location of lymph nodes are important in the staging of the disease and are used to determine the appropriate postoperative adjuvant treatment[3–5].

Initially, mastectomy plus axillary lymph node dissection (ALND) was the standard surgical strategy, but this procedure was associated with postoperative complications. Currently, sentinel lymph node biopsy (SLNB) is the standard of care for lymph node staging in patients with clinically negative LNs or 1–2 positive SLNs confirmed by needle biopsy[6–9].

ACOSOG Z0011, a randomized clinical trial, showed the possibility of omitting ALND in patients with diagnosed lymph node metastases (up to two) and using SLNB, achieving equal overall survival rates in patients receiving breast-conserving therapy (BCT), adjuvant therapy and radiotherapy[9]. However, in the SOUND clinical trial, the authors proved that in patients with small BC and negative preoperative ALNUS results, the omission of axillary surgery was not inferior to SLNB if distant disease-free survival was assessed as the primary endpoint of the study[10].

In the preoperative assessment of ALNs, US is the imaging modality of choice for evaluation and is more accurate than mammography (MMG), magnetic resonance imaging (MRI), positron emission tomography/computed tomography (PET/CT) or PET/MRI[11]. In the Breast Imaging-Reporting and Data System (BIRADS) Atlas, there are missing precise cut-off values for performing LN biopsy in patients with BC, which is problematic in daily practice decision making[12].

According to the literature, ALNUS suspicious findings based on classical B-mode examination and colour Doppler imaging include diffuse or eccentric cortical thickening (more than or equal to 3 mm), complete or partial effacement of the fatty hilum, a rounded shape, a ratio of the long axis to the short axis (L/T) of < 2, and peripheral vascularity[13]. However, according to the literature, the sensitivity and specificity of AUS are 26%-95% and 44%-98%, respectively[14–16], because the US morphological features of benign and malignant LNs often overlap.

[1]Radiology Department II, The Maria Skłodowska-Curie National Research Institute of Oncology, Warsaw, Poland. [2]Department of Ultrasound, Institute of Fundamental Technological Research, Polish Academy of Sciences, Warsaw, Poland. [3]Department of Pathology, The Maria Skłodowska-Curie National Research Institute of Oncology, Warsaw, Poland. ✉email: katarzyna.dobruch-sobczak@pib-nio.pl

Novel imaging techniques that could improve diagnostic accuracy in the differentiation of benign and malignant LNs are being identified. Among other tools, sonoelastography (SE) and small vessel microflow imaging have been investigated. In terms of evaluating the utility of shear wave elastography (SWE), only a few studies have been published. The results showed that quantitative assessment of LN stiffness improves diagnostic sensitivity. [17–19] Moreover, microvascular flow imaging (MVFI) allows the visualization of small vessels with very low velocity flows. This approach relies on detecting Doppler shifts, which remain angle dependent, but reduces noise and other artefacts, improving the sensitivity to slower-flow Doppler signals[20]. In single small-group studies, the authors used this technique and demonstrated a significant difference between malignant and benign LNs[21].

Metastatic lymph nodes often exhibit few suspicious features; therefore, in our study, we evaluated the diagnostic performance of single and multiple B-mode features combined with SWE and MVFI in differentiating between benign and malignant axillary LNs in patients with breast cancer.

Materials and methods

This prospective case–control study was approved by the Ethics Committee of the National Institute of Oncology-Research Institute, Warsaw, and was conducted at the Department of Radiology PIB NIO between November 2021 and April 2023.

Patients.

Axillary lymph node ultrasound (ALNUS) was performed for 99 patients (mean age, 61 ± 13 years; age range, 27–86 years) with 103 confirmed breast cancer tumours (4 women had tumours in the contralateral breasts).

The inclusion criteria for the study are presented in Fig. 1.

The criteria for excluding lymph nodes from the study were as follows:

1. Nonsuspicious according to ultrasound assessment in patients qualified for NAC (neoadjuvant chemotherapy) or.

2. Suspicious according to the ultrasound assessment but with a negative **FNAB/CNB (fine-needle aspiration biopsy/core needle biopsy)** result in patients who qualified for NAC.

The reason for exclusion was the lack of possibility of histopathological correlation of nodes.

Criteria for performing FNAB/**CNB** of lymph nodes:

1. Cortical thickening ≥ 3 mm as a single feature

All lymph node biopsies met the following criteria: **FNAB** and/or core **CNB** were performed before surgery. Postsurgical histopathological verification was used as the reference standard. If the FNAB was negative, the node underwent **CNB**.

Ultrasound acquisition and analysis

Ultrasound B-mode and SWE were performed using an Aixplorer ultrasound system (SuperSonic Imagine, Aix en Provence, France) equipped with a 4–15 MHz linear array transducer. Six experienced breast imaging radiologists (with 5–25 years of experience) performed the examinations. Two radiologists and 1 consultant (K.D.S., 25 years of experience) analysed the images by consensus to eliminate reader variability. The readers

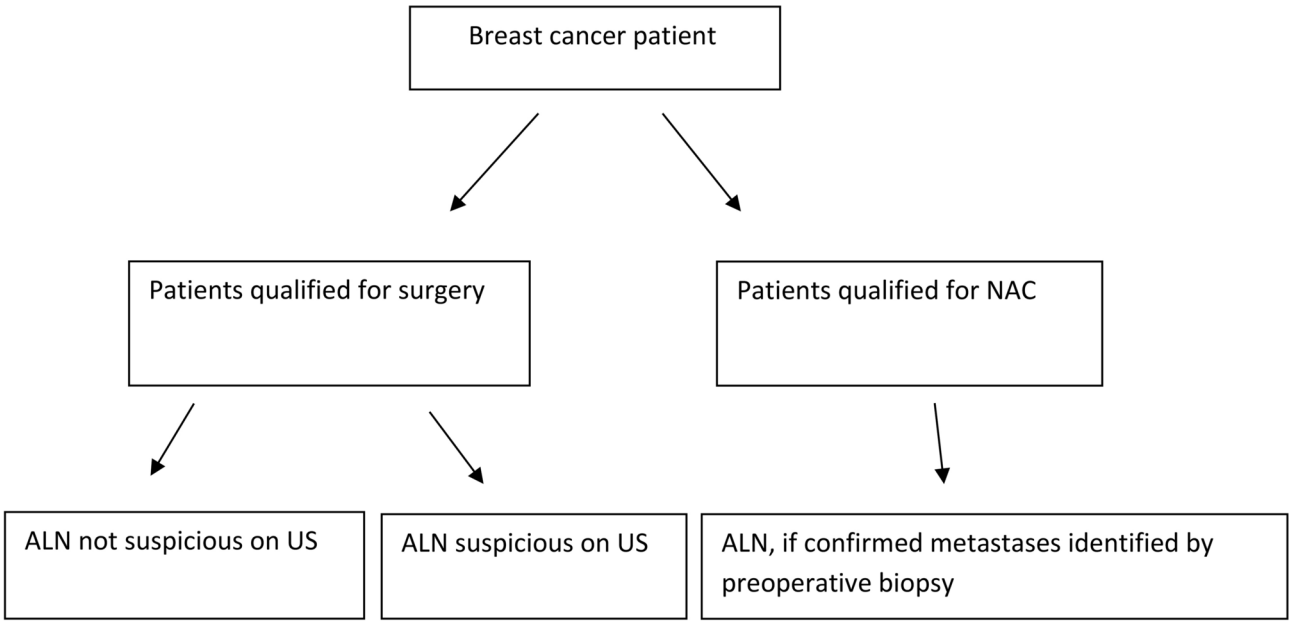

Fig. 1. The inclusion criteria for the study.

were blinded to the pathologic results. B-mode ultrasound was performed on patients in the supine position, with the arms placed above the head. Images were taken in two orthogonal planes (three dimensions) for ALNs.

The parameters assessed by B-mode ultrasound were lymph node short- and long-axis diameter, lymph node shape, cortical thickness with a cut-off point of 3 mm for metastasis, and the presence of a capsule. Vascularity assessment via colour Doppler (CD) included the following: lack of vessels, physiological vessels (vascular tree), perforating/from the capsule or mixed vasculature. Additional AngioPLUS was performed to assess microvascularity in comparison to the CD pattern.

SWE was performed with minimum compression from the probe to identify ALNs that were suspicious or located in the lowest part of the level I.

SWE was used for quantitative assessment. The LNs were in the centre of the field of view (FOV), and the circular box of the system (SWE Q-box SuperSonic Imagine) was placed at the stiffest region of the cortex. The Q-box diameter was related to the cortical thickness of the LNs .The quantitative values, which included the mean (E mean) and maximum (E max) of the elasticity values defined in kPa, were calculated along the longitudinal axis of the ALNs to avoid any anisotropic phenomenon that could influence the stiffness. During the examination, the probe was held steady for a few seconds to stabilize the elastogram, after which the mean value from 2 measurements was measured.

Histopathological/cytological analysis

In all patients, core needle biopsies (**CNBs**) of the breast tumours were performed after the administration of 2% lignocaine. Then, according to the inclusion criteria of the study, **FNAB or CNB** of the lymph nodes was performed. **CNB** was conducted via US-guided core biopsy (14G needle, automatic or semiautomatic). Two to three samples were routinely obtained from the node and preserved in a 10% formalin solution for histological studies embedded in paraffin after fixation. **FNAB** was also performed using a 23G needle under US guidance. The needle was directed accordingly to enter the node at the thickest portion of its cortex. After removal of the needle, the aspirate was expelled forcefully onto 2–4 clean dry slides without delay to avoid clotting of the blood within the hub. At least two aspiration samples were obtained from the selected lymph node. The smears were processed by wet preparations with 95% ethanol and stained with haematoxylin and eosin.The same pathologist, who had 27 years of experience in oncological pathology, assessed the breast tumours and performed the cytology and **CNB** of the ALNs. In all patients, the lymph nodes were assessed after surgery. The sentinel lymph node was identified via radioisotope injection.

Statistical analysis

The statistical analysis was performed with software R: A Language and Environment for Statistical Computing, version 4.1.2. Numeric variables are described as the mean ± SD or median (IQR), depending on the distribution. Normality was checked with the Shapiro–Wilk test and verified with skewness and kurtosis. Variance homogeneity was assessed with Levene's test. Groups with and without metastasis were compared with Student's t test, the t-Welch test, the Mann–Whitney U test, Pearson's chi-square test or Fisher's exact test. Logistic regression was performed to determine which predictors influenced the odds of metastasis and to quantify the strength of the associations. Receiver operating characteristic (ROC) analysis was performed to evaluate the prediction qualities of the analysed variables and their combinations. The optimal cut-off was calculated with the Youden method. All the statistical tests were considered significant when the p value was lower than 0.05.

Results

Description of the study population

Analysis was based on 103 ALNs in 99 patients with BC. Patients with metastasis (mean age 54.1 y) were 5 years younger than patients without metastasis (64.1 y) (MD = -5.30, p = 0.045). The most common immunohistochemical types of BC were luminal A (n = 44), triple negative (n = 20), luminal B HER2- (n = 19), luminal B HER2 + (n = 15), and HER2 + (n = 6). According to the histopathological postoperative verification, 59/103 ALNs exhibited metastasis. Sonographically guided biopsy was performed on 59/103 ALNs that met the following criteria: **CNB** (n = 13) and FNAB (n = 56). Among the biopsied LNs in 10/62 patients, the results were negative, and SLNB was performed. On the other hand, 10 ALNs that did not qualify for biopsy ultimately showed metastasis (micrometastases, n = 3; focus of the metastasis, 3 mm, n = 1; ILC **(invasive lobular carcinoma),** n = 4; NST **(no special type)** BC, n = 2). Among patients with confirmed metastatic LNs, 44 patients were eligible for NAC.

Diagnostic performance of the B-mode ultrasound features

The diagnostic performance of the B-mode ultrasound features is presented in Table 1, and comparisons of patients with and without LN metastasis are listed. Statistical analysis was performed for the whole group and the group with a cortex < 3 mm.

A significant difference in the LN shape was confirmed (p = 0.001). In the group with metastasis, oval shapes were observed less frequently (67.8% vs. 95.5%), while round and irregular shapes were observed more frequently (10.2%, n = 6 vs. 2.3%, n = 1 and 22.0% vs. 2.3%, n = 1, respectively). A cortex less than 3 mm in thickness was significantly less frequent in the group with metastasis (16.9% vs. 77.3%), while a cortex greater than or equal to 3 mm in thickness was significantly more frequent in the group with metastasis (83.1% vs. 22.7%), p < 0.001. The axis length (long/short) was significantly smaller in the group with metastasis (p = 0.011). The structure of the CD type was significantly different between the groups (p < 0.001). CD from the hilum and the absence of CD flow were less frequently observed in the metastasis group (33.9% vs. 70.5% and 13.6%, n = 8 vs. 18.2%, n = 8, respectively). CD perforation and mixed CD were more frequent in the metastasis group (22.0% vs. 6.8%,

Variable	Total group (n = 103)				Cortex < 3 mm (n = 44)			
	With metastasis (n = 59, 57.3%)	Without metastasis (n = 44, 42.7%)	MD (95% CI)	p	With metastasis (n = 10, 22.7%)	Without metastasis (n = 34, 77.3%)	MD (95% CI)	p
Shape								
Oval	40 (67.8)	42 (95.5)	-	0.001[d]	10 (100.0)	34 (100.0)	-	-
Round	6 (10.2)	1 (2.3)			0 (0.0)	0 (0.0)		
Irregular	13 (22.0)	1 (2.3)			0 (0.0)	0 (0.0)		
Shape								
Oval	40 (67.8)	42 (95.5)	-	0.001	10 (100.0)	34 (100.0)	-	-
Round/irregular	19 (32.2)	2 (4.5)			0 (0.0)	0 (0.0)		
Cortex								
< 3 mm	10 (16.9)	34 (77.3)	-	< 0.001	10 (100.0)	34 (100.0)	-	-
≥ 3 mm	49 (83.1)	10 (22.7)			0 (0.0)	0 (0.0)		
Axis (long/short), cm	1.96 ± 0.67	2.50 ± 1.23	−0.54 (−0.95;-0.13)	0.011[b]	2.01 ± 0.67	2.75 ± 1.29	−0.74 (−1.59;0.12)	0.090[a]
CD								
From the hilum	20 (33.9)	31 (70.5)	-	< 0.001	9 (90.0)	27 (79.4)	-	> 0.999[d]
Absent	8 (13.6)	8 (18.2)			1 (10.0)	6 (17.6)		
	13 (22.0)	3 (6.8)			0 (0.0)	0 (0.0)		
Mixed	18 (30.5)	2 (4.5)			0 (0.0)	1 (2.9)		
CD								
From the hilum/absent	28 (47.5)	39 (88.6)	-	< 0.001	10 (100.0)	33 (97.1)	-	> 0.999[d]
Perforating from the capsule/mixed	31 (52.5)	5 (11.4)			0 (0.0)	1 (2.9)		
AngioPLUS								
Even	40 (67.8)	39 (88.6)	-	0.025	8 (80.0)	31 (91.2)	-	0.317[d]
AngioPLUS predominance	19 (32.2)	5 (11.4)			2 (20.0)	3 (8.8)		
Capsule								
Even	20 (33.9)	41 (93.2)	-	< 0.001	8 (80.0)	33 (97.1)	-	0.125[d]
Uneven	39 (66.1)	3 (6.8)			2 (20.0)	1 (2.9)		

Table 1. Characteristics and comparison of patients with and without LN metastasis. Numeric parameters are described as the mean ± standard deviation or as the median (interquartile range), depending on the normality of the distribution. MD – mean/median difference (with metastasis vs. without metastasis), CI – confidence interval. [a]Groups were compared with Student's t test, [b]The t-Welch test, [c]The Mann–Whitney U test, [d]The Pearson chi-square test or Fisher's exact test, As appropriate.

Variable	Total group (n = 103)				Cortex < 3 mm (n = 44)			
	With metastasis (n = 59, 57.3%)	Without metastasis (n = 44, 42.7%)	MD (95% CI)	p	With metastasis (n = 10, 22.7%)	Without metastasis (n = 34, 77.3%)	MD (95% CI)	p
E max, kPa	18.00 (10.00;37.00)	13.50 (8.00;17.00)	4.50 (1.00;13.00)	0.012[c]	15.33 ± 7.37	12.65 ± 6.22	2.69 (−2.20;7.58)	0.274[a]
E mean, kPa	10.00 (5.00;20.00)	10.00 (5.75;13.00)	0.00 (−2.00;4.00)	0.576[c]	11.56 ± 5.79	10.24 ± 5.27	1.32 (−2.75;5.39)	0.516[a]

Table 2. Performance characteristics and comparison of patients with and without LN metastasis, SWE. Numeric parameters are described as the mean ± standard deviation or median (interquartile range), depending on the normality of the distribution. MD – mean/median difference (with metastasis vs. without metastasis), CI – confidence interval. [a]Groups were compared with Student's t test, [b]The t-Welch test, [c]The Mann–Whitney U test, [d]The Pearson chi-square test or Fisher's exact test, As appropriate.

n = 3; 30.5% vs. 4.5%, n = 2, respectively). The prevalence of visible vessels in the AngioPLUS-differentiated groups significantly (p = 0.025). AngioPLUS predominance was more frequent in the metastasis group (32.2% vs. 11.4%, n = 5). Capsule differentiation was significant (p < 0.001), and uneven capsules were observed more frequently in the metastasis group (66.1% vs. 6.8%, n = 3). In the groups of the LNs with a cortex < 3 mm (n = 44) none of the analysed traits significantly differentiated metastatic/non metastatic LNs (p > 0.05) (Table 1).

Diagnostic performance of the quantitative SWE features

When the stiffness of the LN cortex was measured, the E max was significantly greater in the group with metastasis (Table 2).

The Emax in the metastasis group was 4.50 kPa greater than that in the nonmetastasis group (MD = 4.50 CI_{95} [1.00;13.00], p = 0.012).

The E mean not differ between patients with and without metastasis (p > 0.05) (Table 2).

ROC analysis for B-mode and SWE features

ROC analysis was performed for all analysed features and parameters to determine their effectiveness in predicting metastasis as separate variables.

Single US features

The greatest effectiveness in metastasis prediction was observed for cortex and uneven capsule. A cortex greater than or equal to 3 mm resulted in an AUC equal to 0.802 (95% CI: 0.723; 0.881), the sensitivity was 83%, and the specificity was 77%. Using an uneven cortex as a separate predictor of metastasis resulted in an AUC of 0.796 (95% CI: 0.725;0.868), a sensitivity of 66% and a specificity of 93%. ROC analysis of the Emax indicated that the best cut-off was 26.5 kPa, with an AUC of 0.647 (95% CI: 0.540–0.754), a sensitivity of 39% and a specificity of 95%. The E-mean resulted in weaker outcomes than did the E-max. The optimal cut-off was 22.5, and the AUC was 0.533, with a sensitivity of 23% and a specificity of 98%. Mixed CDs were better at predicting metastasis than were perforating CDs from the capsule. The AUCs were 0.630 and 0.576, respectively. The predominance of AngioPLUS resulted in a prediction effevtiveness of an AUC equal to 0.604. The full outcomes of the ROC analysis for the assessed parameters are presented in Table 3.

Logistic regression for B-mode and SWE features

Predictors for logistic regression were B-mode and SWE as well as their combinations. Cortex and capsule were selected as base variables for designing the combinations, while Emax > 26.5 kPa, mixed CD, perforation from the capsule CD and AngioPLUS status were selected as additional variables for creating combinations. Combinations were created as "and" types (feature 1 and feature 2) and as "or" types (feature 1 or feature 2). All possible combinations of two variables, including the cortex or capsule as the first variable and one of the other features as the second variable, were created. Similarly, combinations of three variables were created. All 3-element combinations with AUCs greater than the AUC of each feature considered separately were included in logistic regression analysis as predictors.

In patients group with uneven capsules, the risk of metastasis was nearly 27 × greater than that in patients with even capsules (OR = 26.65, p < 0.001).

In patients with an uneven capsule or cortex greater than or equal to 3 mm or an E max greater than 26.5 kPa, the risk of metastasis was 26 × greater (OR = 26.00, p < 0.001). In patients with uneven capsules, CD perforation from the capsule or an E max above 26.5 kPa, the risk of metastasis was 22 × greater (OR = 21.84, p < 0.001). In patients with uneven capsules or with mixed CD or an E max above 26.5 kPa, the risk of metastasis was 21 × greater (OR = 21.44, p < 0.001). An uneven capsule or cortex greater than or equal to 3 mm increased the risk by 19x (OR = 19.12, p < 0.001). In patients whose cortex was 3 mm or greater, whose CD was perforated from the capsule or whose Emax was greater than 26.5 kPa, the risk of metastasis was 19 × greater (OR = 18.75, p < 0.001). In patients with an uneven capsule or with AngioPLUS predominance or an E max above 26.5 kPa, the risk of metastasis was 18 × greater (OR = 18.30, p < 0.001).

Variable	Cut off*	AUC (95% CI)	Sensitivity	Specificity	Accuracy	PPV	NPV	p
Cortex ≥ 3 mm	-	0.802 (0.723;0.881)	0.83	0.77	0.81	0.83	0.77	< 0.001
Capsule uneven	-	0.796 (0.725;0.868)	0.66	0.93	0.78	0.93	0.67	< 0.001
Perforating from the capsule/mixed	-	0.706 (0.626;0.786)	0.53	0.89	0.68	0.86	0.58	< 0.001
E max > 26.5 kPa	-	0.670 (0.599;0.741)	0.39	0.95	0.63	0.92	0.55	< 0.001
E max, kPa	26.5	0.647 (0.540;0.754)	0.39	0.95	0.63	0.92	0.55	< 0.001
Shape round/irregular	-	0.638 (0.571;0.706)	0.32	0.95	0.59	0.90	0.51	< 0.001
CD mixed	-	0.630 (0.563;0.697)	0.31	0.95	0.58	0.90	0.51	< 0.001
Axis (long/short), cm	1.89	0.630 (0.521;0.740)	0.54	0.70	0.61	0.71	0.53	0.004
Axis (long/short) < 1.89 cm	-	0.623 (0.530;0.717)	0.54	0.70	0.61	0.71	0.53	0.012
AngioPLUS predominance	-	0.604 (0.528;0.681)	0.32	0.89	0.56	0.79	0.49	0.011
E mean > 22.5 kPa	-	0.603 (0.543;0.662)	0.23	0.98	0.55	0.93	0.49	0.001
Shape irregular	-	0.599 (0.541;0.657)	0.22	0.98	0.54	0.93	0.48	0.001
Age, years	53.00	0.598 (0.486;0.709)	0.46	0.82	0.61	0.77	0.53	0.049
CD	-	0.576 (0.511;0.641)	0.22	0.93	0.52	0.81	0.47	0.028
Shape round	-	0.539 (0.495;0.584)	0.10	0.98	0.48	0.86	0.45	0.093
E mean, kPa	22.5	0.533 (0.420;0.646)	0.23	0.98	0.55	0.93	0.49	0.010

Table 3. ROC analysis for predicting metastasis in the overall cohort. AUC – area under curve, CI – confidence interval, PPV – positive predictive value, NPV – negative predictive value. * Cut-off given for numeric variables only.

A cortex greater than or equal to 3 mm was associated with nearly 17 × greater odds of metastasis (OR = 16.66, p < 0.001). In patients with an Emax above 26.5 kPa, the risk of metastasis was increased by 13x (OR = 13.20, p < 0.001). In patients with an E mean above 22.5 kPa, the risk of metastasis increased 13x (OR = 12.70, p = 0.016). An irregular shape increased the odds of metastasis 12x (OR = 12.15, p = 0.018). Mixed CDs were associated with a 9 × greater risk (OR = 9.22, p = 0.004). Perforation from the capsule CD was associated with a 4 × greater risk (OR = 3.86, p = 0.045). AngioPLUS predominance was associated with a 4 × greater risk (OR = 3.70, p = 0.017). An axis length less than 1.89 cm was associated with a 3 × greater risk (OR = 2.83, p = 0.014). CD originating from the hilum and an oval shape were associated with lower odds of metastasis (OR = 0.22, p < 0.001 and OR = 0.10, p = 0.003, respectively; Table 4).

Diagnostic performance of combining quantitative SWE features with conventional US

ROC analysis for metastasis was performed for combinations of features as predictors. Combinations were built as described in logistic regression section. Table 5 summarizes all 3-element combinations with AUCs greater than the AUC of each feature considered separately as well as the respective 2-element combinations for comparative purposes. The AUCs of all those 3-element combinations were greater than 0.800. The greatest AUC was achieved for an uneven capsule or cortex greater than or equal to 3 mm or an E max greater than 26.5 kPa, which was equal to 0.823. The sensitivity of the combination was 90%, and the specificity was 75%. The combination of uneven capsule or mixed CD or an E max greater than 26.5 kPa resulted in an AUC of 0.818, a sensitivity of 77% and a specificity of 86%. The combination of an uneven capsule or perforation from the capsule CD or an E max greater than 26.5 kPa yielded an AUC of 0.812, a sensitivity of 74% and a specificity of 89%. Patients with uneven capsules or a predominant AngioPLUS status or an E max greater than 26.5 kPa and a cortex greater than or equal to 3 mm or perforation from the capsule CD or an E max greater than 26.5 kPa were considered to have a prognosis of metastasis, resulting in AUCs equal to 0.808 and 0.806 respectively.

Discussion

In our study, we applied a multiparameter evaluation of the ALNs based on B-mode US features (shape, cortex, capsule), vascularity (CD and MFI) and stiffness (SWE, E mean and E max value in the cortex) in patients with BC before surgery (Fig. 2, Fig. 3 and Fig. 4). We found that a cortical thickness greater than 3 mm or a noncircumscribed capsular margin of the ALN was the single most suspicious feature suggesting metastasis, with good accuracy and a high PPV. Similar results were published by Abe H et al. and Choi YJ et al. regarding patients with BC before surgery[22,23]. Abe H et al. reported cortical thickening in 63 (79%) of 80 metastatic nodes[22]. Choi YJ et al. revealed in their study that in the multivariate logistic regression analysis, a cortical thickness greater than 3 mm was the most accurate indicator, with a 4.14-fold increased risk of the presence of axillary lymph node metastasis compared to a cortical thickness less than 3 mm (23). In our study, in the cases of nodes with a cortical thickness greater than 3 mm, the vast majority, 83.1%, were characterized by the presence of metastasis; however, in 10/59 ALNs, no metastatic cells were detected (false positive results). On the other hand, in a group of ALNs with a cortex < 3 mm (false negative cases) and in 10/103 patients after

Variable/combination*	OR	95% CI	p
Capsule uneven	26.65	8.38–119.86	< 0.001
Capsule uneven| cortex ≥ 3 mm | E max > 26.5 kPh	26.00	9.35–83.80	< 0.001
Capsule uneven | CD Perforating from the capsule | E max > 26.5 kPh	21.84	7.81–73.08	< 0.001
Capsule uneven | CD mixed | E max > 26.5 kPh	21.44	7.90–67.28	< 0.001
Capsule uneven | cortex ≥ 3 mm	19.12	7.31–55.88	< 0.001
Cortex ≥ 3 mm | CD Perforating from the capsule | E max > 26.5 kPh	18.75	7.16–54.82	< 0.001
Capsule uneven | AngioPLUS predominance | E max > 26.5 kPh	18.30	6.98–54.18	< 0.001
Cortex ≥ 3 mm	16.66	6.53–46.83	< 0.001
E max > 26.5 kPh	13.20	3.55–86.03	< 0.001
E mean > 22.5 kPh	12.70	2.37–235.79	0.016
Shape irregular	12.15	2.27–225.43	0.018
CD mixed	9.22	2.45–60.34	0.004
Shape round	4.87	0.79–93.80	0.150
CD Perforating from the capsule	3.86	1.15–17.71	0.045
AngioPLUS predominance	3.70	1.34–12.06	0.017
Axis (long/short) < 1.89 cm	2.83	1.26–6.61	0.014
CD absent	0.71	0.24–2.09	0.523
CD from the hilum	0.22	0.09–0.49	< 0.001
Shape oval	0.10	0.02–0.38	0.003

Table 4. Logistic regression analysis for determining the risk of metastasis in the total cohort. OR – odds ratio, CI – confidence interval. Outcomes of univariate logistic regression models. *Combinations were built as feature 1, feature 2 or feature 3.

Combination*	AUC (95% CI)	Sensitivity	Specificity	Accuracy	PPV	NPV	p
Capsule uneven | cortex ≥ 3 mm | E max > 26.5 kPa	0.823 (0.747;0.899)	0.90	0.75	0.83	0.83	0.85	< 0.001
Capsule uneven | cortex ≥ 3 mm	0.807 (0.729;0.885)	0.86	0.75	0.82	0.82	0.80	< 0.001
Capsule uneven | E max > 26.5 kPa	0.814 (0.741;0.887)	0.72	0.91	0.80	0.91	0.71	< 0.001
Cortex ≥ 3 mm | E max > 26.5 kPa	0.806 (0.727;0.885)	0.86	0.75	0.81	0.82	0.80	< 0.001
Capsule uneven | CD mixed | E max > 26.5 kPa	0.818 (0.743;0.893)	0.77	0.86	0.81	0.88	0.75	< 0.001
Capsule uneven | CD mixed	0.808 (0.733;0.882)	0.73	0.89	0.80	0.90	0.71	< 0.001
Capsule uneven | E max > 26.5 kPa	0.814 (0.741;0.887)	0.72	0.91	0.8	0.91	0.71	< 0.001
CD mixed | E max > 26.5 kPa	0.735 (0.657;0.813)	0.56	0.91	0.71	0.89	0.62	< 0.001
Capsule uneven | CD perforating from the capsule | E max > 26.5 kPa	0.812 (0.737;0.886)	0.74	0.89	0.80	0.89	0.72	< 0.001
Capsule uneven | CD perforating from the capsule	0.794 (0.720;0.867)	0.68	0.91	0.78	0.91	0.68	< 0.001
Capsule uneven | E max > 26.5 kPa	0.814 (0.741;0.887)	0.72	0.91	0.80	0.91	0.71	< 0.001
CD perforating from the capsule | E max > 26.5 kPa	0.680 (0.599;0.761)	0.47	0.89	0.65	0.84	0.57	< 0.001
Capsule uneven | AngioPLUS predominance | E max > 26.5 kPa	0.808 (0.731;0.885)	0.78	0.84	0.80	0.87	0.74	< 0.001
Capsule uneven | AngioPLUS predominance	0.793 (0.715;0.872)	0.75	0.84	0.79	0.86	0.71	< 0.001
Capsule uneven | E max > 26.5 kPa	0.814 (0.741;0.887)	0.72	0.91	0.80	0.91	0.71	< 0.001
AngioPLUS predominance | E max > 26.5 kPa	0.699 (0.616;0.782)	0.53	0.86	0.68	0.84	0.58	< 0.001
Cortex ≥ 3 mm | CD perforating from the capsule | E max > 26.5 kPa	0.806 (0.727;0.885)	0.86	0.75	0.81	0.82	0.80	< 0.001
Cortex ≥ 3 mm | CD perforating from the capsule	0.802 (0.723;0.881)	0.83	0.77	0.81	0.83	0.77	< 0.001
Cortex ≥ 3 mm | E max > 26.5 kPa	0.806 (0.727;0.885)	0.86	0.75	0.81	0.82	0.80	< 0.001
CD perforating from the capsule | E max > 26.5 kPa	0.680 (0.599;0.761)	0.47	0.89	0.65	0.84	0.57	< 0.001

Table 5. ROC analysis for predicting metastasis in the total group – the most effective 3-element combination. AUC – area under curve, CI – confidence interval, PPV – positive predictive value, NPV – negative predictive value. AUC for combinations of 3 features with AUCs exceeding the AUC of each feature considered separately. Outcomes for combinations of 2 features presented for comparative purposes. *Combinations were built as feature 1, feature 2 or feature 3.

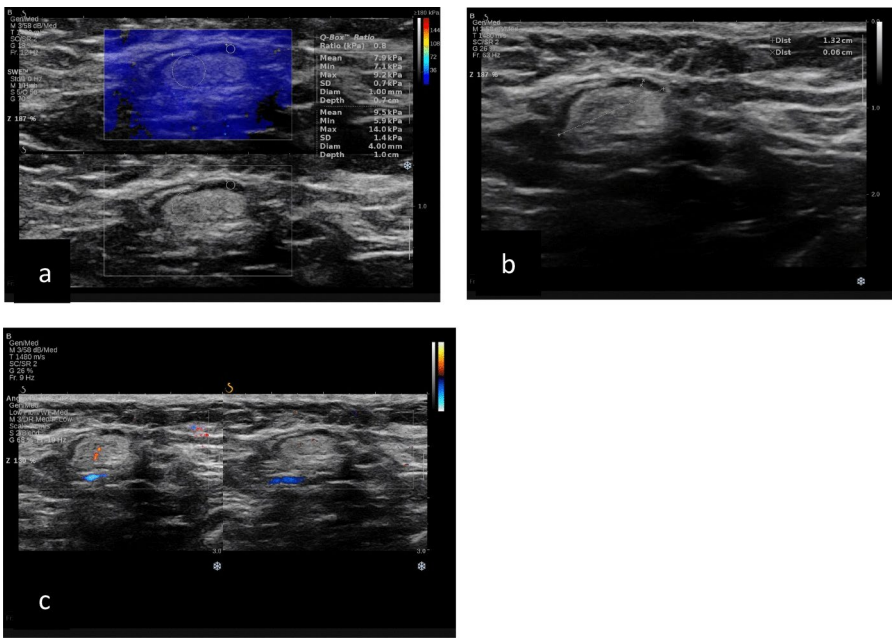

Fig. 2. Non metastatic axillary lymph nodes on US: (a) LN SWE with normal stiffness, E mean 7.9 kPa; (b) B-mode-thin cortex, normal hilum; (c) AngioPLUS small vessel visible in the hilum (on the left), colour Doppler, small vessel in the hilum (on the right).

surgery, metastases were identified. Of these, micrometastases were verified in 3 patients; in one node, the focus of the metastasis was 3 mm, and in 4 patients, these were ILC metastases. In the remaining two patients, the metastasis was classified as BC macrometastasis. When analysing this group of patients, it should be noted that the presence of micrometastases cannot be detected in the ALNUS examination, and their presence does

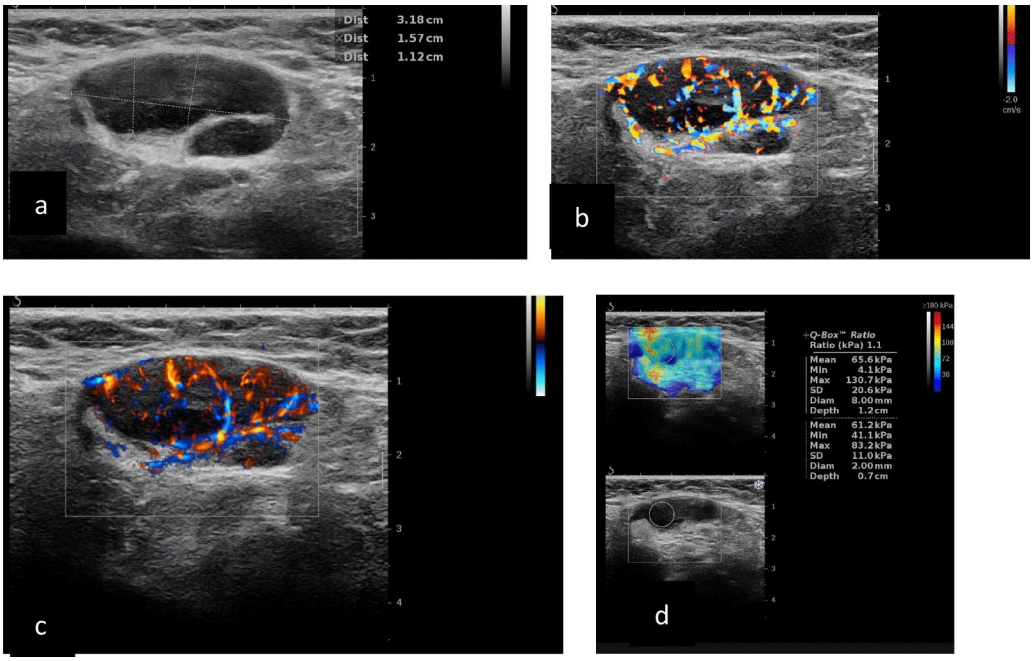

Fig. 3. Metastatic axillary lymph nodes on US examination: (a) LN in the B-mode examination, eccentric thick cortex, and dislocated hilum; (b) colour Doppler image, irregular vessels perforating the capsule, and small vessels in the hilum; (c) AngioPLUS results similar to those of CD; (d) SWE with increased stiffness in the cortex, E mean 65,6 kPa.

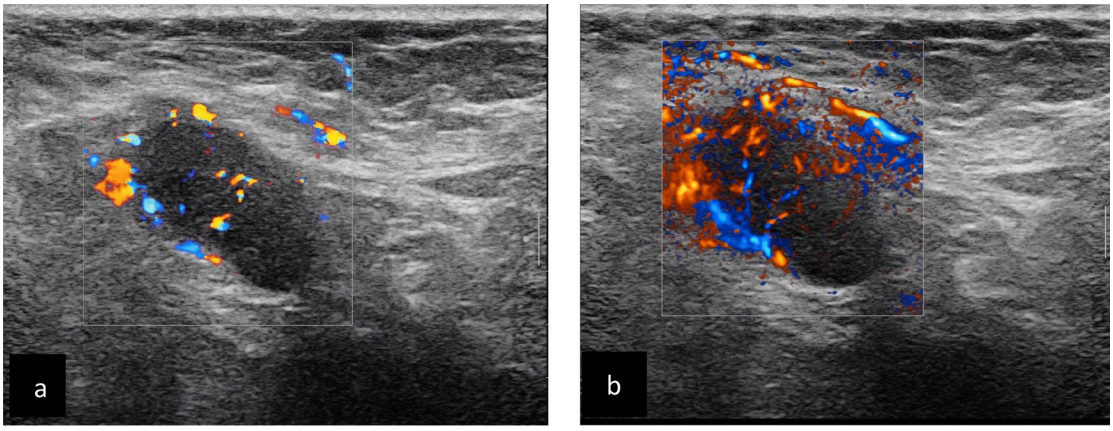

Fig. 4.. Metastatic axillary lymph nodes on US examination: (a) colour Doppler image, irregular vessels perforating the capsule, and small vessels in the hilum; (b) AngioPLUS more pathological vessels are visible comparing to those of CD.

not change the therapeutic procedure. However, in one patient with ILC, failure to visualize the lymph nodes resulted in the patient undergoing another procedure in the axilla. According to the results published by other authors regarding metastatic LNs in BC patients with ILC, Morrow E et al., in a retrospective study using ALNUS in 209 such patients, reported a sensitivity of 32.1% and a very high false negative rate[24]. The authors suggested that in a preoperative assessment of ALNs, biopsy should be performed even if the LN presents as normal in the US examination. Histologically, ILC cells are small and scattered throughout the LN, so at early stages, they do not destroy the architecture of the LN; therefore, it is challenging to detect the metastasis. Kurst et al., who evaluated bladder cancer patients with biopsy-proven metastasis in 219 ALNs, reported that asymmetrical cortical thickening, as a single parameter, was an easy feature to assess via ALNUS, with a sensitivity of 88.7%, specificity of 54.3%, PPV of 77.5%, and NPV of 73.1%[25]. We did not assess these parameters in our study.

In our study, differences in vascularity and stiffness assessed by imaging of the LN were also found as features differentiating their characteristics. Both of these features were characterized by a high PPV but low NPV.

In our study, perforating vessels or mixed vascularity patterns were more common in metastatic LNs than in normal LNs (31/59 vs. 5/44). However, this pattern of vascularity occurred only in approximately half of the LNs with metastases. The absence of vessels was observed only in 16 LNs (8 with metastases in 8 without metastases), so a lack of visible vessels in the LN is not a feature that could differentiate their characteristics.

According to the statistical analysis of the OR, the highest probability of malignancy was obtained for the CD mixed-vascularity pattern (9.2), followed by the perforating pattern (3.9) and the MFVI predominance pattern (3.7). These parameters independently increased the probability of developing lymph node metastases. However, the AUCs for these features in our study were 0.58 and 0.63, respectively. Interesting results were published by Kurt SA et al. on 219 metastatic ALNs. The authors assessed the superb microvascular imaging vascularization pattern of the LN and found that abnormal vascularization (defined as suspicious for metastasis: peripheral, penetrant, anarchic blood supply or avascularity) as a single feature in this metastatic LN had a sensitivity of 79.8, a specificity of 78.6, a PPV of 91.5, an NPV of 57.1, and an AUC of 0.792.

On the other hand, in a study published by Yang WT et al.[26] and Hussien[27], the authors reported that central vascularity patterns were most often observed in benign reactive or inflammatory LNs. Compared with benign axillary LNs, malignant LNs presented greater total and peripheral vessel counts (sensitivity and specificity, respectively). In a study of the measured vascularity index (VI), Uslu et al. used MVFI parameters. The VI is the ratio between the pixels of the Doppler signals and the pixels of the total lesion[21]. The authors reported, based on the 58 LNs (35/58 were metastatic), that this index allows a quantitative assessment of the blood flow richness in the LN. For the cut-off VI of 8.55, the authors reached a sensitivity of 82, a specificity of 100, a PPV of 100, an NPV of 85, and an AUC of 0.91.

In reactively stimulated or normal LNs, Doppler examination revealed visible vessels from the hilum side towards the capsule, with a reduction in their number and diameter (vascular tree). In metastatic nodes, lymphangiogenesis occurs from the lymphatic channels penetrating the node from the capsule side, and peripheral or penetrating vascularization is visible. On the other hand, assessing small vessels using CD and MVFI is limited in deeper organs, and it can be clinically difficult to assess whether the lack of flow detection is because of this depth or whether the flow is not visible in small foci of metastases, which requires further investigation[28]. Nathanson *et* al. reported that lymphatic endothelial cells (LECs) express distinctive lymphatic endothelial markers, such as vascular endothelial growth factor-3, and cytokines that stimulate them[29]. Therefore, malignant cells invade the lymphatic lumen, move with the lymph from the subcapsular sinus to the cortex and proliferate. Tumour cells express VEGF-C and VEGF-D, which are connected with the proliferation of new vessel capillaries (lymphangiogenesis). However, not all tumour cells express chemokine receptors.

Current studies have reported low interobserver variability for SWE and significant improvement in differentiating ALN metastasis from benign ALN metastasis[30]. We also found a significant difference in sonoelastography between benign and metastatic LNs in our study. The best cut-off value was achieved for an E max > 26.5 kPa, which was characterized by a high PPV and specificity but a low NPV and sensitivity. We placed the ROI in the cortex because metastatic cells invade the LNs from the capsula through the afferent lymphatic vessels. In this area of the LNs, the increased density of pathological cells likely increased the stiffness. In the meta-analysis published by Wang R.Y. et al., both shear-wave elastography (SWE) and strain elastography (SE) were used for the assessment of ALNs[31]. Both SE and SWE had relatively high pooled AUCs of 0.85 and 0.94, respectively. The SWE values were significantly greater in malignant LNs. Similar to our study, SWE (maximum stiffness) had a greater AUC than SWE (mean stiffness), and the cut-off values ranged from 20.9 kPa to 38.6 kPa. Seo M et al.evaluated B-mode features and SWE in 54 LNs in BC patients and found significantly greater SWE values for metastatic LNs[19]. The mean values for metastatic LNs were E max = 79.8 kPa and E mean = 55.99 kPa; for benign LNs, the mean values were E max = 13.35 kPa and E mean = 9.38 kPa. However, these results could be explained by LN selection. SWE was performed in LNs where the mean cortical thickness of the metastatic LNs was greater than that in other studies (8.99 mm), and the majority of the metastatic LNs were metastatic (34/54). These results revealed that elastography should be performed during the assessment of LNs and could aid in decision making before biopsy.

Finally, in the multiparametric analysis, which assessed the AUC as well as the OR, the combination of B-mode features (cortex larger than 3 mm, noncircumscribed margin of the LN capsule) and SWE (E max > 26 kPa) for one model and the combination of B-mode features (noncircumscribed margin of the LN capsule), vascular analysis on CD (mixed or penetrating pattern) and SWE (E max > 26 kPa) were superior for determining a single approach. Similar results were reported by Seo M et al., who reported a combined modality (cortical thickness > = 4.85 mm or maximum stiffness > = 20.9 kPa), with an AUC of 0.946.

In the future, we plan to assess patterns of enhancement via CEUS **(contrast-enhanced ultrasound)** as a predictor of malignancy and deep learning methods to improve the preoperative diagnosis of metastatic LNs in patients with BC.

Certainly, our study has some limitations:

First, this study was conducted in women with breast cancer, and consequently, the number of metastatic LNs was high. Second, it was not possible to determine whether the nodes that qualified during US examination to biopsy were exactly the same nodes assessed by the pathologist. We targeted the most suspicious LNs with a cortex larger than 3 mm for biopsy. Another limitation of our study involves the false-negative results, which could be explained by deep LNs being located behind the pectoralis muscles or the small size of the LNs.

Conclusions

This comprehensive study underscores the usefulness of a multiparametric US approach in the evaluation of ALNs. The integration of B-mode US characteristics with modern technology, such as SWE and CD parameters, significantly enhances the diagnostic accuracy required to better differentiate benign and metastatic axillary lymph nodes.

Data Availability

US pictures are stored in Hospital system Clininet and are available from Magdalena Gumowska on reasonable request.

Received: 22 July 2024; Accepted: 17 September 2024
Published online: 04 October 2024

References

1. Chen, M. Y. & Gillanders, W. E. Staging of the Axilla in Breast Cancer and the Evolving Role of Axillary Ultrasound. *Breast Cancer (Dove Med Press)* **13**, 311–323 (2021).
2. Wöckel, A. *et al.* Interdisciplinary Screening, Diagnosis, Therapy and Follow-up of Breast Cancer. Guideline of the DGGG and the DKG (S3-Level, AWMF Registry Number 032/045OL, December 2017) - Part 2 with Recommendations for the Therapy of Primary, Recurrent and Advanced Breast Cancer. *Geburtshilfe Frauenheilkd*. **78,** 1056–1088 (2018).
3. Teichgraeber, D. C., Guirguis, M. S. & Whitman, G.J. Breast Cancer Staging: Updates in the *AJCC Cancer Staging Manual*, 8th Edition, and Current Challenges for Radiologists, From the *AJR* Special Series on Cancer Staging. *AJR Am J Roentgenol*. **217,** 278–290 (2021).
4. Loibl, S. *et al.* Early breast cancer: ESMO Clinical Practice Guideline for diagnosis, treatment and follow-up. *Ann. Oncol.* **35**, 159–182 (2024).
5. Chang, J. M., Leung, J. W. T., Moy, L., Ha, S. M. & Moon, W. K. Axillary Nodal Evaluation in Breast Cancer: State of the Art. *Radiology* **295**, 500–515 (2020).
6. Krag, D. N. *et al.* Sentinel-lymph-node resection compared with conventional axillary-lymph-node dissection in clinically node-negative patients with breast cancer: overall survival findings from the NSABP B-32 randomised phase 3 trial. *Lancet Oncol.* **11**, 927–933 (2010).
7. Burak, W. E. et al. Sentinel lymph node biopsy results in less postoperative morbidity compared with axillary lymph node dissection for breast cancer. *Am J Surg.* **183**, 23–27 (2002).
8. Brackstone, M. *et al.* Management of the Axilla in Early-Stage Breast Cancer: Ontario Health (Cancer Care Ontario) and ASCO Guideline. *J Clin Oncol.* **39**, 3056–3082 (2021).
9. Giuliano, A. E. *et al.* Effect of Axillary Dissection vs No Axillary Dissection on 10-Year Overall Survival Among Women With Invasive Breast Cancer and Sentinel Node Metastasis: The ACOSOG Z0011 (Alliance) Randomized Clinical Trial. *JAMA* **318**, 918–926 (2017).
10. Gentilini, O. D. *et al.* Sentinel Lymph Node Biopsy vs No Axillary Surgery in Patients With Small Breast Cancer and Negative Results on Ultrasonography of Axillary Lymph Nodes: The SOUND Randomized Clinical Trial. *JAMA Oncol.* **9**, 1557–1564 (2023).
11. Marino, M. A., Avendano, D., Zapata, P., Riedl, C. C. & Pinker, K. Lymph Node Imaging in Patients with Primary Breast Cancer: Concurrent Diagnostic Tools. *Oncologist25*, 231–242 (2020).
12. Mendelson, E. B. *et al. ACR BI-RADS® Ultrasound. In: ACR BI-RADS® Atlas, Breast Imaging Reporting and Data System* (American College of Radiology, 2013).
13. Ecanow, J. S., Abe, H., Newstead, G. M., Ecanow, D. B. & Jeske, J. M. Axillary staging of breast cancer: what the radiologist should know. *Radiographics* **33**, 1589–1612 (2013).
14. Riedel, F. *et al.* Diagnostic accuracy of axillary staging by ultrasound in early breast cancer patients. *Eur J Radiol.* **135**, 109468 (2021).
15. Alvarez, S. *et al.* Role of sonography in the diagnosis of axillary lymph node metastases in breast cancer: a systematic review. *AJR Am J Roentgenol.* **186**, 1342–1348 (2006).
16. Lee, B. *et al.* The efficacy of axillary ultrasound in the detection of nodal metastasis in breast cancer. *AJR Am J Roentgenol.* **200**, 314–320 (2013).
17. Kilic, F. *et al.* Ex Vivo Assessment of Sentinel Lymph Nodes in Breast Cancer Using Shear Wave Elastography. *J Ultrasound Med.* **35**, 271–277 (2016).
18. Luo, S. *et al.* Qualitative Classification of Shear Wave Elastography for Differential Diagnosis Between Benign and Metastatic Axillary Lymph Nodes in Breast Cancer. *Front Oncol.* **9**, 533 (2019).
19. Seo, M. & Sohn, Y. M. Differentiation of benign and metastatic axillary lymph nodes in breast cancer: additive value of shear wave elastography to B-mode ultrasound. *Clin Imaging* **50**, 258–263 (2018).
20. Aziz, M. U. *et al.* Microvascular Flow Imaging: A State-of-the-Art Review of Clinical Use and Promise. *Radiology* **305**, 250–264 (2022).
21. Uslu, H. & Tosun, M. The benefit of superb microvascular imaging and shear wave elastography in differentiating metastatic axillary lymphadenopathy from lymphadenitis. *Clin Breast Cancer* **22**, 515–520 (2022).
22. Abe, H. *et al.* Axillary lymph nodes suspicious for breast cancer metastasis: sampling with US-guided 14-gauge core-needle biopsy–clinical experience in 100 patients. *Radiology.* **250**, 41–49 (2009).
23. Choi, Y. J. *et al.* High-resolution ultrasonographic features of axillary lymph node metastasis in patients with breast cancer. *Breast.* **18**, 119–122 (2009).
24. Morrow, E. *et al.* Population-based study of the sensitivity of axillary ultrasound imaging in the preoperative staging of node-positive invasive lobular carcinoma of the breast. *Br J Surg.* **105**, 987–995 (2018).
25. Aladag, Kurt, S. et al. Predicting axillary nodal metastasis based on the side of asymmetrical cortical thickening in breast cancer: Evaluation with grayscale and microvascular imaging findings. *Eur J Radiol.* **158**, 110643 (2023).
26. Yang, W. T., Chang, J. & Metreweli, C. Patients with breast cancer: differences in color Doppler flow and gray-scale US features of benign and malignant axillary lymph nodes. Radiology. 215, 568–573 (2000). 27. Yang, W. T., Metreweli, C., Lam, P. K. & Chang, J. Benign and malignant breast masses and axillary nodes: evaluation with echo-enhanced color power Doppler US. *Radiology*. **220**, 795–802 (2001).
27. Hussien, A. R., El-Quadi, M. & Oconnell, A.Value of ultrasound in evaluation of abnormal axillary lymph nodes. *American Journal of Sonography*. **4**, (2021).
28. Vullings, J. J. J., Schaik, C. V., Fütterer, J. J., de Korte, C. L. & Klein, W. M. Visualizing the lymphatic vessels and flow with high-resolution ultrasonography and microvascular flow imaging. *Ultrasonography.* **42**, 466–473 (2023).
29. Nathanson, S. D. Insights into the mechanisms of lymph node metastasis. *Cancer.* **98**, 413–423 (2003).
30. Berg, W. A. *et al.* Shear-wave elastography improves the specificity of breast US: the BE1 multinational study of 939 masses. *Radiology.* **262**, 435–449 (2012).
31. Wang, R. Y., Zhang, Y. W., Gao, Z. M. & Wang, X. M. Role of sonoelastography in assessment of axillary lymph nodes in breast cancer: a systematic review and meta-analysis. *Clin Radiol.* **75**, 320 (2020).

Acknowledgements

To the team of surgeons and oncologists caring for the patients included in this study, and Marta Nowak, who

was responsible for the statistical analysis.

Author contributions

Author contributions: conceptualization, K.D-S methodology, K.D-S investigation, K.D-S, A.Sz, MG, JM, KF, EŁ data curation, K.D-S, A.Sz, MG writing—original draft preparation, K.D-S, JM, MJ writing—review and editing, K.D-S, JM, MG, MJ, KF, EŁ review and pathological consultation, KR-P All authors have read and agreed to the published version of the manuscript.

Declarations

Competing interests

The authors declare no competing interests.

Ethical approval

All procedures performed in studies involving human participants were in accordance with the ethical standards of the institutional and/or national research committee and with the 1964 Helsinki declaration and its later amendments or comparable ethical standards.

Human with animal rights

This article does not contain any studies with animals performed by any of the authors.

Informed consent

Informed consent was obtained from all individual participants included in the study.

Additional information

Correspondence and requests for materials should be addressed to K.D.-S.